blood®
Regular Article

RED CELLS, IRON, AND ERYTHROPOIESIS

Disrupting CD147-RAP2 interaction abrogates erythrocyte invasion by *Plasmodium falciparum*

Meng-Yao Zhang,[1-4,*] Yang Zhang,[1,3,*] Xiao-Dong Wu,[1,3,*] Kun Zhang,[1,3,5,*] Peng Lin,[1,3,*] Hui-Jie Bian,[1,3] Min-Min Qin,[1] Wan Huang,[1,3] Ding Wei,[1,3] Zhao Zhang,[1,3] Jiao Wu,[1,3] Ruo Chen,[1,3] Fei Feng,[1,3] Bin Wang,[1,3] Gang Nan,[1,3] Ping Zhu,[1,2] and Zhi-Nan Chen[1,3]

[1]National Translational Science Center for Molecular Medicine, [2]Department of Clinical Immunology, Xijing Hospital, and [3]Department of Cell Biology, Fourth Military Medical University, Xi'an, China; [4]Beijing Institute of Biotechnology, Beijing, China; and [5]College of Life Science and Bioengineering, School of Science, Beijing Jiaotong University, Beijing, China

KEY POINTS

- **The CD147-RAP2 interaction is essential for erythrocyte invasion by *P falciparum* and is independent from the known interactions involved.**
- **HP6H8, which specifically interrupts the CD147-RAP2 pair, is capable of complete elimination and prevention of *P falciparum* infection in humanized mice.**

Effective vaccines against malaria caused by *Plasmodium falciparum* are still lacking, and the molecular mechanism of the host-parasite interaction is not fully understood. Here we demonstrate that the interaction of RAP2, a parasite-secreted rhoptry protein that functions in the parasitophorous vacuole formation stage of the invasion, and CD147 on the host erythrocyte is essential for erythrocyte invasion by *P falciparum* and is independent from all previously identified interactions involved. Importantly, the blockade of the CD147-RAP2 interaction by HP6H8, a humanized CD147 antibody, completely abolished the parasite invasion with both cure and preventative functions in a humanized mouse model. Together with its long half-life on human red blood cells and its safety profile in cynomolgus monkeys, HP6H8 is the first antibody that offers an advantageous approach by targeting a more conserved late-stage parasite ligand for preventing as well as treating severe malaria. (*Blood*. 2018;131(10):1111-1121)

Introduction

Malaria is a deadly epidemic infectious disease.[1-3] The emergence of parasites that are resistant to chemical drugs such as chloroquine[4] and the core artemisinin component[5] and the lack of effective vaccines are the main barriers to eliminating malaria, largely because of polymorphism and resistance mutations in the rapidly evolving *Plasmodium* genome and the absence of adequately developed immunologic memory.[6,7] In addition, many chemical drugs are not suitable for use in pregnant women and children because of severe adverse effects, and vaccines, in order to be effective, require proper immune responses, which are lacking in children and immunocompromised patients.[8-10] Therefore, there is an urgent need to develop better and safer drugs such as antibodies.

Erythrocyte invasion by *Plasmodium falciparum* is essential to the life cycle of the parasite and is central to malaria pathogenesis.[11,12] Parasite invasion involves 4 major steps: initial contact, reorientation, tight junction (TJ) motility, and parasitophorous vacuole (PV) formation and is controlled by interactions between multiple secreted parasite ligands with cognate receptors on the host cells in an orderly manner.[13-15] The primary contact, when merozoites attach to an erythrocyte, is reported to be mediated via merozoite surface proteins.[16] The reorientation stage is thought to be mediated by merozoite ligands released from apical organelles to erythrocytes, including 2 ligand families, *P falciparum* reticulocyte-binding protein homologs (PfRhs) and erythrocyte-binding–like proteins.[17-20] Among those, 4 receptor-ligand pairs, glycophorin A-EBA175,[21] glycophorin C-EBA140,[22-24] complement receptor 1 (CR1)-PfRh4,[25] and CD147-PfRh5[11,26,27] are involved at this stage, of which the CD147-PfRh5 interaction is the only one that is essential for the parasite invasion. The TJ formation and motility involve 2 parasite-secreted proteins, *P. falciparum* apical membrane antigen (PfAMA1) and rhoptry neck protein 2 (RON2), to form an AMA1-RON2 complex.[15] The PV is formed as the merozoite is pulled into the erythrocyte by the actomyosin motor during which the rhoptry bulb proteins that play important roles during internalization are released[13]. However, the molecular mechanism and the interactions in the PV formation are not fully understood.

Of the rhoptry bulb proteins, rhoptry-associated proteins (RAPs) are a group of proteins released to form the PV and are composed of RAP1, RAP2, and RAP3.[28,29] Among them, RAP2 has been a favorable candidate for malaria vaccine because of its low degree of genetic polymorphism,[30] its recognition by sera

from patients living in endemic areas,[31] its link with red blood cell (RBC) destruction and bone marrow suppression associated with malarial anemia,[32] and its essential function for parasite survival as demonstrated by unsuccessful attempts at genetic deletion.[33] Studies have shown that peptides derived from RAP2 with erythrocyte-binding ability can block merozoite invasion in vitro, and recombinant RAP2 is capable of inducing protective antibody responses in vivo.[34,35] However, the exact roles that RAP2 and its receptors play on RBCs remain unknown.[28,34]

In this study, we identified RAP2 as a ligand of CD147 expressed on RBCs; their interaction is essential for parasite invasion, and they function at a later stage in the parasite invasion, independent of the previously identified CD147-PfRh5 pair.[11,26,27] More importantly, we demonstrated that HP6H8, a humanized monoclonal antibody against CD147 that specifically interrupts the CD147-RAP2 interaction, potently blocked the parasite invasion in vitro and in vivo, which may provide both curative and preventative functions in an immune-response independent way for malaria control. HP6H8 may be adapted for travelers and inhabitants of epidemic areas and may also meet the special needs of pregnant women, children, and immunocompromised patients.

Methods

P falciparum culture and invasion assays

P falciparum parasite strains were cultured in human O-positive erythrocytes in complete medium. Invasion assays were carried out in 96-well plates at a hematocrit level of 2%. Ring-form parasites were mixed with antibodies or peptides and incubated for 72 hours. Two methods were used for achieving parasitemia. For the growth inhibition assay (GIA) of HP6H8, Giemsa-stained thin blood films were viewed under a microscope. For the GIA of the CD147 peptide, parasitemia was measured by SYBR Green I staining (Invitrogen; S7563), and the newly added RBCs were labeled by using CellTrace Far Red,[36,37] with a BD LSRFortessa flow cytometer for data acquisition.

Therapeutic efficacy of HP6H8 in humanized mice

NOG (NOD/Shi-scid/IL-2Rγnull) mice were purchased from Beijing Vitalstar Biotechnology. All experiments were performed under specific-pathogen-free conditions. The mice were treated according to the experimental animal protocols that were approved by the Institutional Animal Care and Use Committee.

Eleven-week-old NOG mice were intravenously injected with human RBCs (huRBCs) suspended in human serum. Parasitemia was measured by viewing Giemsa-stained thin blood films once per day. Parasites were considered to be eliminated when parasitemia was below 1/10 000.[38-40] The huRBCs were labeled by anti-human CD235a (Glycophorin A) phycoerythrin and mouse IgG2b κ Isotype Control phycoerythrin (12-9987, 12-4732; BD Biosciences), and the engrafting rates were measured by flow cytometry.

Mice engrafted with huRBCs were randomly divided into various groups according to weights and engrafting rates. HP6H8 was administrated to treatment groups. Saline and a human immunoglobulin G (IgG) protein were administered to placebo and control groups, respectively.

Immunoaffinity chromatography and mass spectrometry

Immunoaffinity chromatography was performed with Affi-Gel Hz Immunoaffinity Kit (Bio-Rad Laboratories, Hercules, CA). Silver staining with sodium dodecyl sulfate polyacrylamide gel electrophoresis gels was performed by using Pierce Silver Stain for Mass Spectrometry Kits. Trypsin-digested protein samples were analyzed with LTQ-Orbitrap XL (Thermo Fisher Scientific) mass spectrometry.

Surface plasmon resonance

(SPR) measurements were performed by using a ProteOn XPR36 protein interaction array system (Bio-Rad Laboratories) with a general layer compact sensor chip. Immobilized samples were coupled onto the activated channels, and the reaction was terminated with ethanolamine HCl. After a brief wash, protein samples were simultaneously injected into the chip. Bovine serum albumin (BSA) protein was used as the control protein, and the BSA signal was deducted during analysis of the kinetic parameters by ProteOn Manager Version 2.0 software (BioRad Laboratories).

For the interruption experiments by SPR, CD147 protein was incubated with the Fab fragment of 6H8 to form a CD147-6H8Fab complex. Then the complex was isolated by size exclusion chromatography. The CD147-6H8Fab complex was injected onto the chip immobilized with BSA, RAP2, and PfRh5 proteins separately. The interaction between peptides and proteins was conducted by using the Biacore T200 system (GE Healthcare Life Sciences) with a CM5 chip.

Co-immunoprecipitation

A coimmunoprecipitation (Co-IP) experiment was performed using a Pierce Co-IP Kit (Thermo Fisher Scientific). The following antibodies were used: rabbit anti-FLAG (F7425; Sigma-Aldrich), mouse anti-6X His tag (Sigma-Aldrich, SAB2702218), anti-CD147 (produced in our laboratory), and anti-RAP2 (produced from a 3A9/48 hybridoma; BEI Resources).

Adhesion tests

huRBCs were incubated with or without 6H8Fab. RAP2-HIS protein was then added. Adhesion was detected by using anti-HIS rabbit antibody and visualized with fluorescein isothiocyanate fluorescent secondary antibody with a BD LSRFortessa flow cytometer (BD Biosciences).

Crystallization, data collection, and structure determination

Purified CD147D1-6H8Fab complex was crystallized in 0.2 M lithium sulfate monohydrate and 20% (w/v) PEG3350 at 16°C via the hanging drop vapor diffusion method. X-ray diffraction data for the complex crystals were collected at 100 K at the beamline 19-ID (Advanced Photon Source, Argonne National Laboratory). A 2.3-Å resolution data set was integrated and scaled by using the HKL2000 Program.[41] The complex structure was determined by molecular replacement with the CD147 ectodomain (Protein Data Bank [PDB] entry: 3B5H) and mouse antibody Fab (PDB entry: 5H90) searching model using Phenix Phaser. The initial model containing 2 CD147D1-6H8Fab protein complexes was

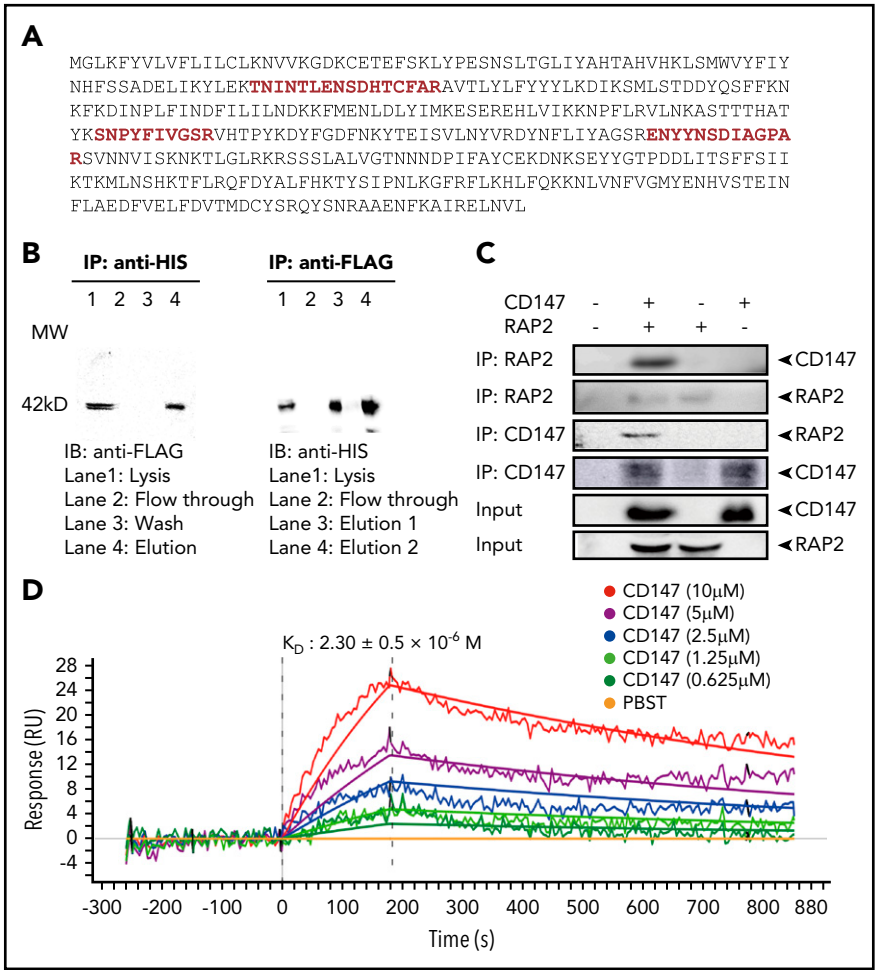

Figure 1. CD147 and RAP2 interaction. (A) The full length of the RAP2 protein sequence with mass spectrometry–identified peptide sequences highlighted in red. (B) Western blots showing Co-IP of CD147 and RAP2 overexpressed in HEK-293 cells. CD147 is HIS-tagged and RAP2 is FLAG-tagged. Reciprocal pull-down and detection results are shown. (C) Western blots showing Co-IP of CD147 and RAP2 protein purified from *Escherichia coli*. Reciprocal Co-IP and detection results are shown. (D) The binding affinity of RAP2 to CD147 by SPR. The calculated K_D value is shown as mean ± standard deviation (SD). RU, response units.

refined by making manual adjustments with the crystallographic object-oriented toolkit (Coot)[42] and a general purpose crystallographic structure refinement program (PHENIX.Refine).[43]

Electron microscopy

huRBCs were incubated with or without 6H8 antibody before the Pf3d7 parasites were added. The infected cells were fixed with glutaric dialdehyde/polyoxymethylene buffer polymerized with 1% agar. The embedded cell masses were cut into thin slices and placed on nickel grids. The grids were then stained with uranyl acetate and lead citrate. Microscopic observations were made by using a JEM-1400 microscope (JEOL, Tokyo, Japan).

Results

RAP2 is a ligand of CD147

Previous studies by Crosnier et al showed that CD147 is a receptor of the parasite ligand PfRh5, and the CD147-PfRh5 interaction is essential for the initial contact and reorientation during erythrocyte invasion.[26,27] Interestingly, the same group reported that some of the anti-CD147 antibodies showed potent growth inhibition activities but did not inhibit the CD147-PfRh5 interaction,[44] consistent with similar findings observed for some of the antibodies from our laboratory. It is conceivable that there may be a separate ligand(s) that might interact with CD147 for the parasite invasion. This motivated us to search for such ligands.

Lysate of RBCs infected by 2 *P falciparum* strains, Nf54 and FCC1, was incubated with an anti-CD147 antibody immobilized on an affinity gel. Purified proteins were separated and visualized by silver-stained sodium dodecyl sulfate polyacrylamide gel electrophoresis. The detected protein bands were gel excised and digested with trypsin, followed by analysis using mass spectrometry. Several peptides were identified whose sequences matched the RAP2 sequences (Figure 1A), indicating that RAP2 may be associated with CD147. To confirm this finding, RAP2 was co-expressed with CD147 in HEK-293 cells, and the lysate was used to perform Co-IP. Data clearly demonstrated that the CD147-RAP2 complex formed when CD147 and RAP2 were co-expressed (Figure 1B). To provide additional evidence for the CD147-RAP2 interaction, RAP2 was expressed and purified from *Escherichia coli*, and the purified RAP2 was tested for its direct interaction with CD147. The results again showed formation of the CD147-RAP2 complex (Figure 1C).

To further verify this direct interaction, an SPR test was performed. The RAP2 protein was immobilized on the chip, and CD147 was injected. Both kinetic and equilibrium binding parameters for the interaction were derived by using a 1:1 binding model, and they were in excellent agreement. The calculated binding constant (K_D) value was $2.3 \pm 0.5 \times 10^{-6}$ M, typical of extracellular protein interactions measured by using this technique,[45] and the χ^2 value of every experiment was below 10 (Figure 1D).

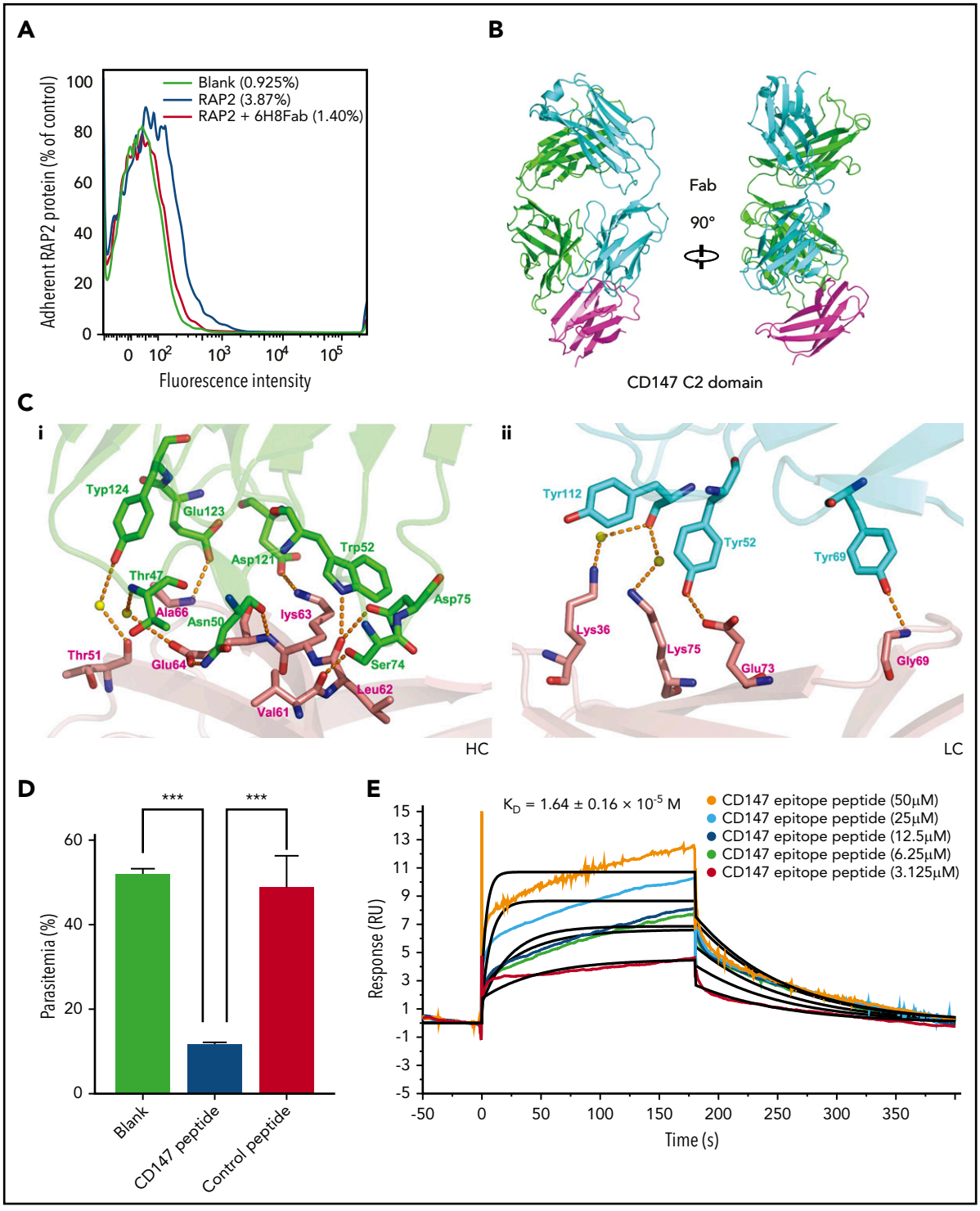

Figure 2. Disruption of the CD147-RAP2 interaction by 6H8. (A) The overlaid flow cytometry assays of the protein-cell adhesion tests. The blank control (black), RAP2 binding to red blood cells (blue), and the reversal of the binding by 6H8Fab (red). The adhesion was detected by anti-HIS rabbit antibody and visualized with fluorescein isothiocyanate fluorescent secondary antibody by flow cytometer. (B) The crystal structure of the CD147D1-6H8Fab complex. (C) Detailed CD147D1-6H8Fab interface. (Ci) For the heavy chain of 6H8, the CD147 binding interface is located at a groove formed by CDR-H1, -H2, and -H3, where D1-βC′ (^{61}VLKEDA^{66}) is half buried in the groove, resulting in 3 hydrogen bonds between D1-βC′ and the heavy chain. (Cii) Binding of CD147D1 to the light chain of 6H8 is weaker than that to its heavy chain, where 2 hydrogen bonds exist between the D1-βE and the light chain of 6H8; no hydrophobic interaction was observed. (D) The invasion assay of the CD147 peptide derived from the CD147-6H8 interface epitope against *P falciparum* 3D7 strain in vitro (n = 3). The control peptide represents the randomized sequence of the CD147 peptide. For data acquisition, parasitemia was measured by SYBR Green I staining with a flow cytometer. Values are mean ± standard error of the mean (SEM). (E) The binding kinetics of the CD147-derived peptide to RAP2 by SPR. The calculated K_D value is shown as mean ± SD. *P* values were calculated by using the analysis of variance test. ***$P < .0001$.

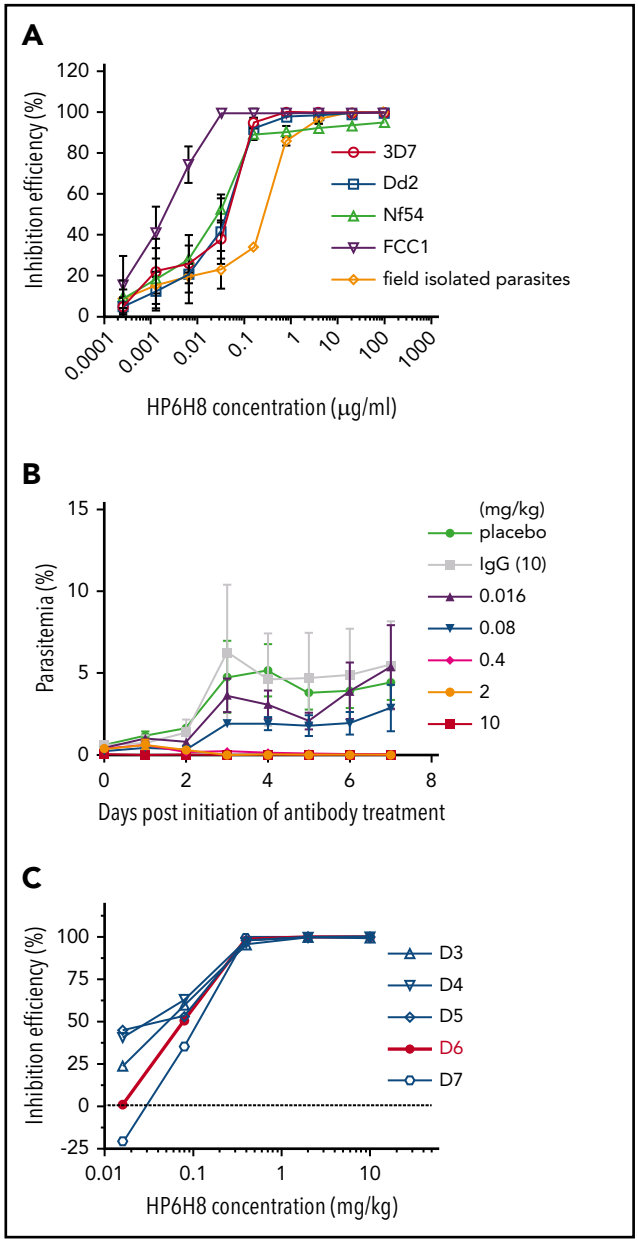

Figure 3. The inhibition efficacy of HP6H8 against *P falciparum*. (A) In vitro invasion assay of HP6H8 against *P falciparum* strains (Dd2, 3D7, FCC1, and Nf54) and parasites isolated from the field (n = 3). (B) Parasitemia after administration of HP6H8 in huRBC-engrafted NOG mice. Lines show doses of HP6H8 at 0.016, 0.08, 0.4, 2, and 10 mg/kg, placebo group, and IgG 10 mg/kg group (n = 5, 3, 6, 6, 5, 4, and 4, respectively). Data shown are mean ± SD. (C) Inhibition efficacy of HP6H8 in humanized mice. Red line represents the best fitting curve.

6H8 specifically disrupts CD147-RAP2 interaction

To further understand the CD147-RAP2 interaction at the molecular level and to develop a way to probe the biological functions of this interaction, an anti-CD147 antibody, 6H8, with a K_D value of 10^{-10} M (supplemental Figure 1 available at the *Blood* Web site) was tested for its ability to disrupt this interaction. Given the close association of RAP2 with RBC-surface-expressed CD147, it follows that RAP2 would bind to RBCs. The adhesion of RAP2 to huRBCs was demonstrated by fluorescence-labeled cells, and this adhesion was completely reversed by pre-incubating RBCs with 6H8Fab, the Fab fragment of 6H8 (Figure 2A). An SPR test also demonstrated the specific disruption of the CD147-RAP2 complex. In this experiment, CD147 and 6H8Fab were pre-incubated, and the CD147-6H8Fab complex that was formed was purified by size exclusion chromatography. The purified complex was then injected onto chips on which the RAP2 protein and the PfRh5 protein were immobilized. Although binding to CD147 by RAP2 was completely blocked by the complex formation, binding to CD147 by PfRh5 was totally unaffected (the K_D value of the interaction between CD147-6H8Fab and PfRh5 remained at 10^{-6} M; supplemental Figure 2), indicating that 6H8 blocked only the CD147-RAP2 interaction.

The disruption of the CD147-RAP2 interaction by 6H8 may be achieved either by 6H8-induced conformational changes of CD147 or by competitive binding to the same or overlapping epitopes of RAP2. The extracellular domain of CD147 is composed of 2 Ig-like domains. Preliminary experiments indicated that 6H8 interacted only with the N-terminal Ig-like domain (CD147D1). We co-crystallized CD147D1 with 6H8Fab and determined the crystal structure of the CD147D1-6H8Fab complex at a resolution of 2.3Å (PDB entry: 5X0T; Figure 2B; supplemental Table 1). The epitope for 6H8 is mainly composed of 2 β strands and a connecting loop, encompassing amino acids 61-75 (^{61}VLKEDALPGQKTEFK^{75}) in CD147D1 (Figure 2C). This peptide was then chemically synthesized and used to perform invasion inhibition tests and RAP2 binding tests. A peptide with the same amino acid composition but a scrambled sequence (LKQVKPELETDAFKG) was used as a negative control. Peptide 61-75 exhibited significant invasion inhibition (Figure 2D), and its affinity with RAP2 was determined by SPR with a K_D of 10^{-5} M (Figure 2E). Taken together, these data demonstrated that 6H8 specifically inhibited RAP2 binding to CD147 by competitive binding to the same or similar epitopes.

HP6H8 inhibits erythrocyte invasion in vitro and cures *P falciparum* infection in humanized mice

Several experiments were designed to determine the biological significance of the CD147-RAP2 interaction. First, HP6H8, a humanized version of 6H8, was used in an in vitro GIA, and the results showed that HP6H8 has potent activity against multiple strains of *P falciparum*, including 3D7, Dd2, Nf54, FCC1, and a parasite isolated from the blood of a patient from Yunnan, China (Figure 3A). The 50% effective inhibitory concentration (EC_{50}) values ranged from 1.81 to ~31.64 ng/mL for the laboratory isolates and the EC_{50} was ~0.17 μg/mL for the unsynchronized patient-derived parasite.

To demonstrate the pharmacodynamic activity of HP6H8, we used NOG mice engrafted with huRBCs as an in vivo model system. In this model, mice were infused with huRBCs with an engrafting rate of ~100% which lasted for more than 30 days. The parasitemia rates could reach as high as 40%, and all stages of parasites existed in murine peripheral blood after infection. The parasitemia rates of the animals dosed at different levels of HP6H8 were determined, and the data showed clear dose-dependent responses with the complete inhibition of the parasite growth at dosing levels as low as 2 mg/kg (Figure 3B). The inhibition efficiency at different dosing levels was also plotted for multiple days. The results from day 6 exhibited a best fitting curve (Figure 3C), with the 50% reduction in parasitemia (ED_{50}) of 79.4 μg/kg (95% confidence interval [CI], 77.1-81.7 μg/kg) and 90% reduction in parasitemia (ED_{90} of 198.1 μg/kg (95% CI, 186.2-209.3 μg/kg).

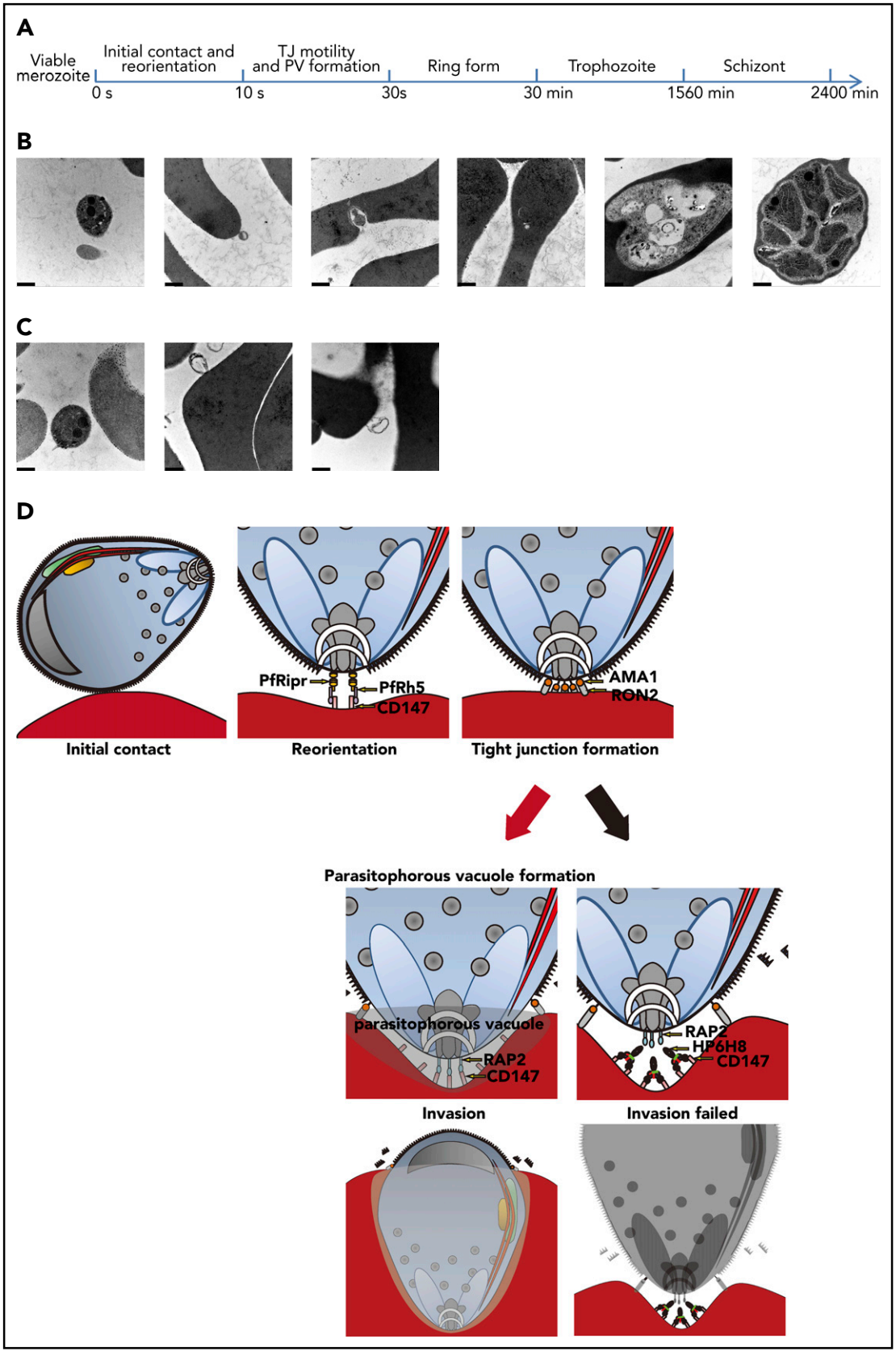

Figure 4. Merozoites invasion with or without HP6H8 treatment. (A) Timeline of the merozoite invasion process in this study. (B) The development of merozoites during invasion in normal conditions observed with a TEM. Scale bar, 500 nm. (C) Merozoite invasion after HP6H8 treatment observed with a TEM. Scale bar, 500 nm. (D) Model of key receptors and ligands participating in the invasion process. (Black arrow) HP6H8 stopped PV formation by blocking the interaction between CD147 and RAP2.

Giemsa-stained thin blood films were examined once per day for 28 days, and no reappearance was observed.

HP6H8 stops merozoite invasion after initial contact and reorientation stages

Next, we determined the stage of the parasite invasion at which the CD147-RAP2 interaction is involved. Viable merozoites of *P falciparum* were added to RBCs that had been pre-incubated with or without HP6H8, and the ultrastructure was then examined by using a transmission electron microscope (TEM) (Figure 4A). We observed that in the absence of HP6H8, merozoites were able to invade RBCs and completed their asexual life cycle: merozoites showed normal apical rest within 10 seconds and formed PVs within 30 seconds. After that, the ring-form parasites were observed at 30 minutes, and the trophozoites were seen at 26 hours, and schizonts were detected at 40 hours[46] (Figure 4B). However, in the presence of HP6H8, most merozoites stopped invasion at 10 seconds, corresponding to the end of the initial contact and reorientation before internalization as previously reported,[47] with 83% of parasites (25 of 30) displaying normal apical resting but abnormal morphologies. As time passed, the parasites showed loosened structures and eventually died (Figure 4C). These results are consistent with the in vitro and in vivo inhibition assays in which the antibody eliminated the parasites completely after 2 life cycles in the blood stage (72 to 96 hours). Our research demonstrated that merozoite invasion was stopped after the initial contact and reorientation stages. An ideograph was used to depict the critical interaction pairs during the erythrocyte invasion process and the mode of action by HP6H8 (Figure 4D).

HP6H8 shows preventive functions in a humanized mouse model

As an alternative approach to using vaccines, we tested HP6H8 for its preventative effects. As shown in Figure 5A, a single injection of HP6H8 at different doses was conducted on day −1 in the huRBC-engrafted NOG mice, followed by the first *P falciparum* infection on day 0 and the second infection on day 10. The data are presented in Figure 5B-C. For the first infection, the data from day 4 exhibited the best fitting curve with an ED_{50} of 0.19 mg/kg (95% CI, 0.13-0.28 mg/kg); the ED_{90} was 0.62 mg/kg (95% CI, 0.47-0.86 mg/kg), with the complete elimination of the parasites achieved at 2 and 10 mg/kg within 3 and 2 days, respectively (Figure 5B). For the second challenge, the data from day 15 (day 5 after the second infection) exhibited the best fitting curve with an ED_{50} of 0.50 mg/kg (95% CI, 0.27-0.75 mg/kg) and an ED_{90} of 0.86 mg/kg (95% CI, 0.69-0.98 mg/kg), with complete elimination of the parasites achieved at 2 and 10 mg/kg within 9 and 3 days after the second infection, respectively (Figure 5C). The differences in ED_{50} and time to complete elimination between the 2 challenges are mainly the reflection of the RBC-binding antibody levels resulting from the antibody's clearance over time. Protection was maintained for 1 month, and the thin blood films showed no recrudescence of parasites.

Pharmacokinetics of HP6H8 in a humanized mouse model

To better understand the protection efficacy and pharmacokinetics of HP6H8, a single intravenous injection study of HP6H8 at 1 mg/kg and 10 mg/kg was performed in huRBC-engrafted mice or nonengrafted mice. At 1 mg/kg, the maximum serum concentrations (C_{max}) of HP6H8 in engrafted mice and nonengrafted mice were 17.53 μg/mL and 24.92 μg/mL, respectively, and the apparent volumes of distribution (V_d) were 61.68 mL/kg and 61.96 mL/kg, respectively, suggesting a main distribution of HP6H8 in the vascular system. The serum elimination half-lives ($t_{1/2}$) of HP6H8 in engrafted and nonengrafted mice were 40.35 hours and 209.46 hours, respectively, suggesting a sink effect of the engrafted mice as a result of the antibody binding to huRBCs. When the dose was raised to 10 mg/kg, the $t_{1/2}$ of HP6H8 was 75.12 hours in the engrafted mice (Figure 5D). Conversely, the data showed that the huRBC-bound HP6H8 could persist for more than 600 hours if it was maintained in a stable condition in the first 400 hours (Figure 5E), which is likely the basis for the long-term effect observed for this antibody.

Acute toxicity study of HP6H8 in cynomolgus monkeys

Anti-CD147 antibodies have been demonstrated to be generally safe in preclinical studies and in some cases for human use.[48,49] To further evaluate the safety of HP6H8, an acute toxicity study was performed. HP6H8 was intravenously administered to cynomolgus monkeys at doses of 30 mg/kg and 100 mg/kg. The results from that study showed that HP6H8 was well tolerated (supplemental Figure 3). No animals died or developed abnormal clinical symptoms, nor were any adverse effects on body temperature, body weight, food consumption, electrocardiogram, clinical chemistry indicators, or immune function observed during the study. The hematology and coagulation tests showed that the percent of reticulocytes increased, although the change was not significant. On day 14, the hematology and coagulation indicators of several monkeys had returned to normal levels. Therefore, the mild abnormal results were transient and recoverable.

Discussion

Patients become resistant to drugs for malaria treatment over time, and some drugs are unsuitable for pregnant women and infants. Great efforts have been made to develop vaccines, but success has been limited. In this report, we identified RAP2 as a ligand of CD147 and determined that the interaction between them is essential for parasite invasion. We further demonstrated that the CD147-RAP2 interaction pair, being completely independent of the previously identified CD147-PfRh5 pair essential for initial contact and reorientation, exerts its pivotal function in the formation of PVs. More importantly, the data presented here demonstrate that HP6H8, a humanized monoclonal antibody against CD147, not only potently and completely eliminated the parasites in the infected animals, but also effectively prevented the animals from being infected when administered before infection in an huRBC-engrafted animal model.

That the CD147-RAP2 interaction is essential was demonstrated by the complete blockage of erythrocyte invasion by HP6H8 specifically disrupting the CD147-RAP2 interaction and is consistent with and supported by previous failed attempts to generate RAP2 mutations.[33] It is also demonstrated by the TEM results. By ultrastructure analysis of the parasite invasion process, we found that although the parasite invasion proceeded normally in the early steps (initial contact and reorientation), the merozoites died in the later stages of the invasion process in the

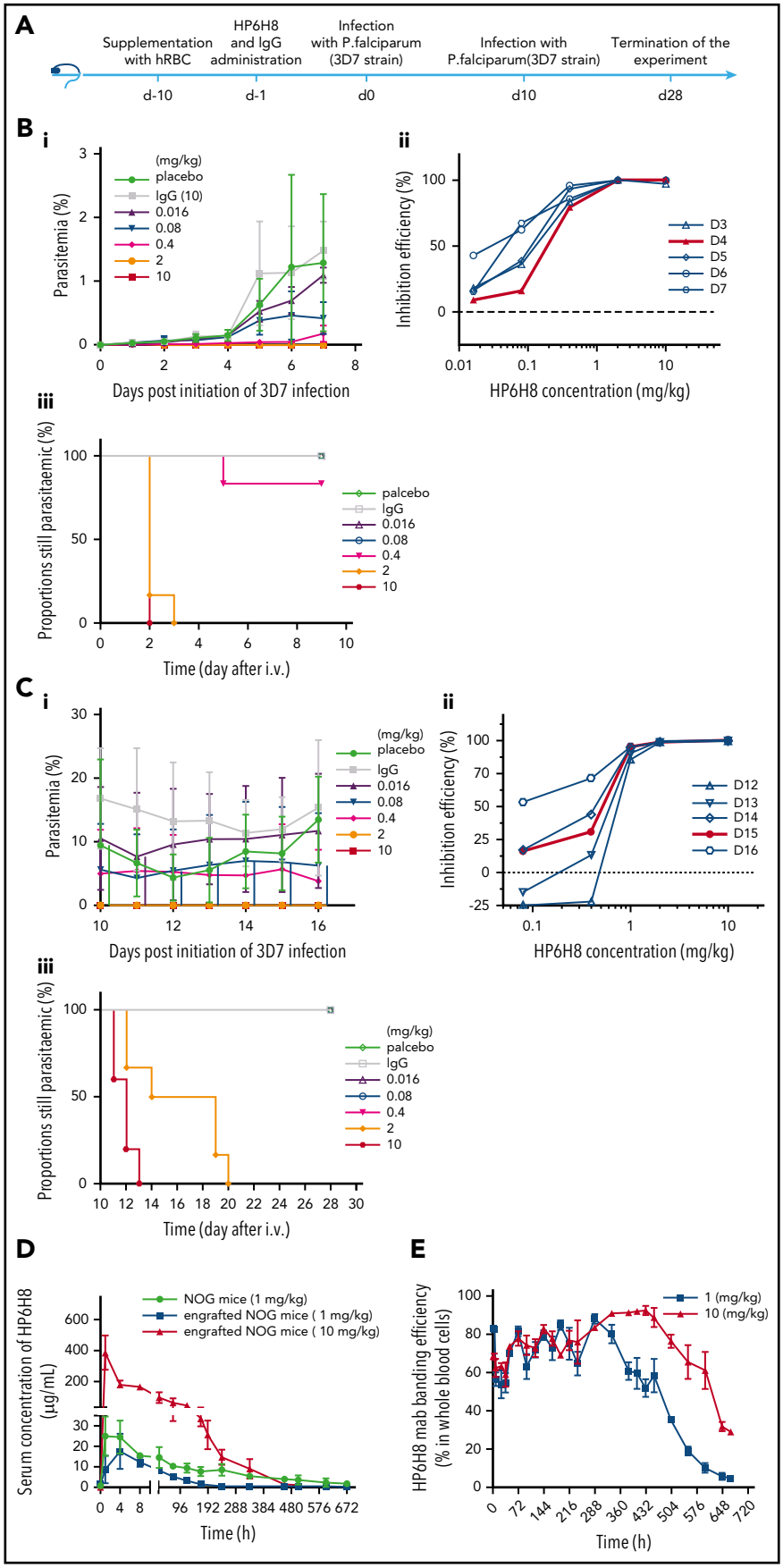

Figure 5. Prevention efficacy and pharmacokinetics of HP6H8. (A) Schedule of the prevention challenge tests in huRBC-engrafted NOG mice. (Bi) Parasitemia, (Bii) inhibition efficacy, and (Biii) the proportion of mice remaining parasitemic after the first *P falciparum* infection. (Bi-Bii) Lines show doses of HP6H8 at 0.016, 0.08, 0.4, 2, and 10 mg/kg, placebo group, and IgG 10-mg/kg group (n = 3, 4, 6, 6, 6, 6, and 4, respectively). (Biii) Proportion still parasitemic was analyzed by survival analysis, which showed the clean time of the complete elimination of parasites in mice with doses of HP6H8 at 0.016, 0.08, 0.4, 2, and 10 mg/kg, placebo group, and IgG group (n = 5, 5, 6, 6, 6, 8, and 6, respectively). (Ci) Parasitemia and (Cii) inhibition efficacy after the second infection with doses of HP6H8 at 0.016, 0.08, 0.4, 2, and 10 mg/kg, placebo group, and IgG group (n = 5, 5, 6, 6, 5, 5, and 3, respectively). (Ciii) Survival analysis of the proportion of mice remaining parasitemic; n = 6 for HP6H8 at 0.016 mg/kg and placebo groups; n = 5 for other groups. (D) Concentrations of HP6H8 in serum of engrafted and nonengrafted mice. (E) Positive rates of HP6H8-binding RBCs in engrafted mice.

presence, but not in the absence, of HP6H8 (Figure 4D). Furthermore, the synthesized epitope mimic based on the crystal structure (peptide 61-75 of CD147) exhibited interaction with RAP2 and showed significant inhibition of the parasite invasion in vitro.

The independence of the CD147-RAP2 interaction from the CD147-PfRh5 interaction is supported by or consistent with the fact that the crystal structures of the CD147-PfRh5[11] and CD147-6H8 have been determined and the CD147 epitopes of the 2 interactions are protruding in opposite directions (extended Figure 1). The temporal and sequential secretion of PfRh5 and RAP2 reported in the literature shows that the CD147-PfRh5 complex participated in the initial contact and reorientation stage during erythrocyte invasion,[50] which occurs upstream of TJ formation,[11,26,27] whereas RAP2 is secreted after TJ formation.[28] This is consistent with and supported by our TEM results. The possible existence of an alternative mechanism was suggested by an earlier report in which 2 anti-CD147 antibodies that did not block CD147-PfRh5 showed potent inhibition activities.[44] The observed efficacy seen with blockade of CD147-RAP2 was 3 orders of magnitude higher than that of CD147-PfRh5 in a similar in vitro growth inhibition assay.[48] Interestingly, even though both CD147-PfRh5 and CD147-RAP2 interactions are essential for parasite invasion, the inhibition efficacies are significantly different, with blocking CD147-RAP2 being approximately 3 orders of magnitude more potent than blocking CD147-PfRh5.

The unprecedented efficacy seen with HP6H8 is likely attributed to the criticality of its targeted CD147-RAP2 interaction in the parasite life cycle identified in this study and to the different time windows and/or stages involved in the invasion process.[44,48] Targeting an essential CD147-RAP2 interaction in the later stages of erythrocyte invasion may also offer other advantages. One advantage is that RAP2 is under less selection pressure during parasite evolution and is therefore more conserved, which was demonstrated by the lack of polymorphism of RAP2 and of being well conserved in different *Plasmodium* species whereas PfRh5 is relatively more polymorphic and is even absent in some *Plasmodium* species. In addition, our finding that the ligand-receptor interaction is essential for the later invasion process indicates that the continuous specific and active engagement between the parasite and host beyond initial contact and reorientation is necessary for the completion of the life cycle of the parasite, which provides a wider window for attacking the parasite for disease control.

Because the studies were performed by repeated infusions of fresh huRBCs while diluting the HP6H8-bound huRBCs at the same time, the actual protection time could be longer than what was shown in this study. The observed differences in time to complete elimination after the 2 separate infections after a single HP6H8 injection were explained partly by normal clearance and partly by the artificial removal of the antibody. An experiment is now under way to assess the RBC-binding half-life of HP6H8 using monkeys with RBC-binding properties similar to those of huRBCs.

An antibody-based approach for treating and preventing malaria is complementary to and may even have an advantage over traditional vaccines in that it is independent of the patient's immune responses and does not involve any chemical drugs that may not be suitable for special populations such as pregnant women and children. In one scenario, a dose of HP6H8 can be given to travelers or individuals at high risk of being exposed to parasite infection. The combination of high efficacy and the long RBC-binding life of HP6H8 could provide full protection for at least 1 month or maybe even longer while allowing time for the patients' own immune system to rebuild after a *P falciparum* infection. This may require fine-tuning the dosing levels for protecting and priming the immune system at the same time.

A potential risk of using an antibody directed at huRBCs is that it may lead to hemolytic anemia or immune-mediated elimination of red blood cells during infection or inflammation. This question was addressed by several experiments listed in supplemental Table 1 and shown in supplemental Figures 4 and 5. The results indicated that the antibody treatment would not lead to hemolytic anemia nor would it induce immune-mediated elimination of red blood cells during infection or inflammation.

More work needs to be done before the HP6H8 antibody and the derived small peptide are ready for testing in humans. The pharmacokinetic studies, safety evaluation, and toxicokinetic studies in monkeys are under way and will be described in future articles. The main challenge associated with this mode of treatment is that intravenous injection may not be convenient in regions where the public medical facilities and faculties are insufficient. Therefore, a subcutaneous injection preparation may be needed and is under evaluation.

Acknowledgments

The authors thank BEI Resources for providing the 3A9/48 hybridoma, the volunteers and field staff involved in sample collections, Wei-Qing Pan (Second Military Medical University), Hong-Quan Wang (Institute of Biotechnology), Duan-Qing Pei (Guangzhou Institutes of Biomedicine and Health, Chinese Academy of Sciences), Wen Yin and Chen Chen (Xijing Hospital of the Fourth Military Medical University), and Jing Ma (National Shanghai Center for New Drug Safety Evaluation) for their technical and material assistance.

This work was supported by a National Science and Technology Major Project grant (2013ZX09301301), the National Basic Research Program of China (2015CB553701), and the China Postdoctoral Science Foundation (2017M613317).

Authorship

Contribution: Z.-N.C., P.Z., and M.-Y.Z. designed experiments, wrote the paper, and discussed the results; M.-Y.Z. performed research and analyzed the data; K.Z. performed in vivo experiments; X.-D.W. performed in vivo experiments, obtained samples, and made the figures; P.L. determined the crystal structure of the complex; Y.Z. and G.N. assisted with using the electron microscope and other instruments; F.F. performed the surface plasmon resonance experiments; B.W. provided the antibodies; H.-J.B. and M.-M.Q. discussed the results and revised the manuscript; and W.H., D.W., Z.Z., J.W., and R.C. discussed the results and commented on the manuscript.

Conflict-of-interest disclosure: The authors declare no competing financial interests.

Patent number for HP6H8 is PCT/CN2017/082713.

The crystal structure of the CD147 D1-6H8Fab complex can be obtained from the Protein Data Bank (PDB entry: 5X0T).

Correspondence: Zhi-Nan Chen, National Translational Science Center for Molecular Medicine, Fourth Military Medical University, No. 169, Changle West Rd, Xi'an 710032, People's Republic of China; e-mail: znchen@fmmu.edu.cn; and Ping Zhu, Department of Clinical Immunology, Xijing Hospital,

Fourth Military Medical University, No. 169, Changle West Rd, Xi'an 710032, People's Republic of China; e-mail: zhuping@fmmu.edu.cn.

*M.-Y.Z., Y.Z., X.-D.W., K.Z., and P.L. contributed equally to this study.

The online version of this article contains a data supplement.

The publication costs of this article were defrayed in part by page charge payment. Therefore, and solely to indicate this fact, this article is hereby marked "advertisement" in accordance with 18 USC section 1734.

Footnotes

Submitted 21 August 2017; accepted 8 January 2018. Prepublished online as *Blood* First Edition paper, 19 January 2018; DOI 10.1182/blood-2017-08-802918.

REFERENCES

1. World Health Organization. World Malaria Report 2016. Geneva, Switzerland: World Health Organization; 2016
2. World Health Organization. World Malaria Report 2015. Geneva, Switzerland: World Health Organization; 2015
3. World Health Organization. World Malaria Report 2014. Geneva, Switzerland: World Health Organization; 2014
4. Veiga MI, Dhingra SK, Henrich PP, et al. Globally prevalent PfMDR1 mutations modulate Plasmodium falciparum susceptibility to artemisinin-based combination therapies. *Nat Commun*. 2016;7:11553.
5. Ariey F, Witkowski B, Amaratunga C, et al. A molecular marker of artemisinin-resistant Plasmodium falciparum malaria. *Nature*. 2014; 505(7481):50-55.
6. Miles A, Iqbal Z, Vauterin P, et al. Indels, structural variation, and recombination drive genomic diversity in Plasmodium falciparum. *Genome Res*. 2016;26(9):1288-1299.
7. Krzych U, Zarling S, Pichugin A. Memory T cells maintain protracted protection against malaria. *Immunol Lett*. 2014;161(2): 189-195.
8. Dahl EL, Shock JL, Shenai BR, Gut J, DeRisi JL, Rosenthal PJ. Tetracyclines specifically target the apicoplast of the malaria parasite Plasmodium falciparum. *Antimicrob Agents Chemother*. 2006;50(9):3124-3131.
9. van Vugt M, Brockman A, Gemperli B, et al. Randomized comparison of artemether-benflumetol and artesunate-mefloquine in treatment of multidrug-resistant falciparum malaria. *Antimicrob Agents Chemother*. 1998; 42(1):135-139.
10. Mordmüller B, Surat G, Lagler H, et al. Sterile protection against human malaria by chemoattenuated PfSPZ vaccine. *Nature*. 2017; 542(7642):445-449.
11. Wright KE, Hjerrild KA, Bartlett J, et al. Structure of malaria invasion protein RH5 with erythrocyte basigin and blocking antibodies. *Nature*. 2014;515(7527):427-430.
12. Galaway F, Drought LG, Fala M, et al. P113 is a merozoite surface protein that binds the N terminus of Plasmodium falciparum RH5. *Nat Commun*. 2017;8:14333.
13. Gaur D, Chitnis CE. Molecular interactions and signaling mechanisms during erythrocyte invasion by malaria parasites. *Curr Opin Microbiol*. 2011;14(4):422-428.
14. Richard D, MacRaild CA, Riglar DT, et al. Interaction between Plasmodium falciparum apical membrane antigen 1 and the rhoptry neck protein complex defines a key step in the erythrocyte invasion process of malaria parasites. *J Biol Chem*. 2010;285(19): 14815-14822.
15. Delgadillo RF, Parker ML, Lebrun M, Boulanger MJ, Douguet D. Stability of the Plasmodium falciparum AMA1-RON2 Complex Is Governed by the Domain II (DII) Loop. *PLoS One*. 2016;11(1):e0144764.
16. Kadekoppala M, Holder AA. Merozoite surface proteins of the malaria parasite: the MSP1 complex and the MSP7 family. *Int J Parasitol*. 2010;40(10):1155-1161.
17. Riglar DT, Richard D, Wilson DW, et al. Super-resolution dissection of coordinated events during malaria parasite invasion of the human erythrocyte. *Cell Host Microbe*. 2011; 9(1):9-20.
18. Singh S, Alam MM, Pal-Bhowmick I, Brzostowski JA, Chitnis CE. Distinct external signals trigger sequential release of apical organelles during erythrocyte invasion by malaria parasites. *PLoS Pathog*. 2010;6(2): e1000746.
19. Tham WH, Healer J, Cowman AF. Erythrocyte and reticulocyte binding-like proteins of Plasmodium falciparum. *Trends Parasitol*. 2012;28(1):23-30.
20. Weiss GE, Gilson PR, Taechalertpaisarn T, et al. Revealing the sequence and resulting cellular morphology of receptor-ligand interactions during Plasmodium falciparum invasion of erythrocytes. *PLoS Pathog*. 2015; 11(2):e1004670.
21. Wanaguru M, Crosnier C, Johnson S, Rayner JC, Wright GJ. Biochemical analysis of the Plasmodium falciparum erythrocyte-binding antigen-175 (EBA175)-glycophorin-A interaction: implications for vaccine design. *J Biol Chem*. 2013;288(45): 32106-32117.
22. Zerka A, Rydzak J, Lass A, et al. Studies on immunogenicity and antigenicity of baculovirus-expressed binding region of Plasmodium falciparum EBA-140 merozoite ligand. *Arch Immunol Ther Exp (Warsz)*. 2016; 64(2):149-156.
23. Zerka A, Rydzak J, Lass A, et al. Erratum to: studies on immunogenicity and antigenicity of baculovirus-expressed binding region of Plasmodium falciparum EBA-140 merozoite ligand. *Arch Immunol Ther Exp (Warsz)*. 2016; 64(2):157.
24. Rydzak J, Kaczmarek R, Czerwinski M, et al. The baculovirus-expressed binding region of Plasmodium falciparum EBA-140 ligand and its glycophorin C binding specificity. *PLoS One*. 2015;10(1):e0115437.
25. Lim NT, Harder MJ, Kennedy AT, et al. Characterization of inhibitors and monoclonal antibodies that modulate the interaction between Plasmodium falciparum adhesin PfRh4 with its erythrocyte receptor complement receptor 1. *J Biol Chem*. 2015;290(42): 25307-25321.
26. Volz JC, Yap A, Sisquella X, et al. Essential role of the PfRh5/PfRipr/CyRPA complex during Plasmodium falciparum invasion of erythrocytes. *Cell Host Microbe*. 2016;20(1):60-71.
27. Crosnier C, Bustamante LY, Bartholdson SJ, et al. Basigin is a receptor essential for erythrocyte invasion by Plasmodium falciparum. *Nature*. 2011;480(7378):534-537.
28. Counihan NA, Kalanon M, Coppel RL, de Koning-Ward TF. Plasmodium rhoptry proteins: why order is important. *Trends Parasitol*. 2013;29(5):228-236.
29. Sterkers Y, Scheidig C, da Rocha M, Lepolard C, Gysin J, Scherf A. Members of the low-molecular-mass rhoptry protein complex of Plasmodium falciparum bind to the surface of normal erythrocytes. *J Infect Dis*. 2007;196(4): 617-621.
30. Saul A, Cooper J, Hauquitz D, et al. The 42-kilodalton rhoptry-associated protein of Plasmodium falciparum. *Mol Biochem Parasitol*. 1992;50(1):139-149.
31. Stowers A, Taylor D, Prescott N, Cheng Q, Cooper J, Saul A. Assessment of the humoral immune response against Plasmodium falciparum rhoptry-associated proteins 1 and 2. *Infect Immun*. 1997;65(6):2329-2338.
32. Seder RA, Chang LJ, Enama ME, et al; VRC 312 Study Team. Protection against malaria by intravenous immunization with a nonreplicating sporozoite vaccine. *Science*. 2013; 341(6152):1359-1365.
33. Baldi DL, Good R, Duraisingh MT, Crabb BS, Cowman AF. Identification and disruption of the gene encoding the third member of the low-molecular-mass rhoptry complex in Plasmodium falciparum. *Infect Immun*. 2002;70(9): 5236-5245.
34. López R, Valbuena J, Curtidor H, et al. Plasmodium falciparum: red blood cell binding studies using peptides derived from rhoptry-associated protein 2 (RAP2). *Biochimie*. 2004;86(1):1-6.
35. Collins WE, Walduck A, Sullivan JS, et al. Efficacy of vaccines containing rhoptry-associated proteins RAP1 and RAP2 of Plasmodium falciparum in Saimiri boliviensis monkeys. *Am J Trop Med Hyg*. 2000;62(4):466-479.
36. Theron M, Hesketh R, Subramanian S, Rayner JC. An adaptable two-color flow cytometric assay to quantitate the invasion of erythrocytes by Plasmodium falciparum parasites. *Cytometry A*. 2010;77(11):1067-1074.
37. Theron M, Hesketh RL, Subramanian S, Rayner JC. An adaptable two-color flow cytometric assay to quantitate the invasion of

erythrocytes by Plasmodium falciparum parasites. *Cytometry A*. 2010;77(11):1067-1074.

38. Fraser CC, Chen BP, Webb S, van Rooijen N, Kraal G. Circulation of human hematopoietic cells in severe combined immunodeficient mice after Cl2MDP-liposome-mediated macrophage depletion. *Blood*. 1995;86(1): 183-192.

39. van Rooijen N, van Kesteren-Hendrikx E. "In vivo" depletion of macrophages by liposome-mediated "suicide". *Methods Enzymol*. 2003; 373:3-16.

40. van Rooijen N, Hendrikx E. Liposomes for specific depletion of macrophages from organs and tissues. *Methods Mol Biol*. 2010;605: 189-203.

41. Otwinowski Z, Minor W. Processing of X-ray diffraction data collected in oscillation mode. *Methods Enzymol*. 1997;276:307-326.

42. Emsley P, Lohkamp B, Scott WG, Cowtan K. Features and development of Coot. *Acta Crystallogr D Biol Crystallogr*. 2010;66(Pt 4): 486-501.

43. Adams PD, Afonine PV, Bunkóczi G, et al. PHENIX: a comprehensive Python-based system for macromolecular structure solution. *Acta Crystallogr D Biol Crystallogr*. 2010; 66(Pt 2):213-221.

44. Douglas AD, Williams AR, Knuepfer E, et al. Neutralization of Plasmodium falciparum merozoites by antibodies against PfRH5. *J Immunol*. 2014;192(1):245-258.

45. Wright GJ. Signal initiation in biological systems: the properties and detection of transient extracellular protein interactions. *Mol Biosyst*. 2009;5(12):1405-1412.

46. Bannister LH, Hopkins JM, Fowler RE, Krishna S, Mitchell GH. A brief illustrated guide to the ultrastructure of Plasmodium falciparum asexual blood stages. *Parasitol Today*. 2000; 16(10):427-433.

47. Harvey KL, Gilson PR, Crabb BS. A model for the progression of receptor-ligand interactions during erythrocyte invasion by Plasmodium falciparum. *Int J Parasitol*. 2012;42(6): 567-573.

48. Zenonos ZA, Dummler SK, Müller-Sienerth N, et al. Basigin is a druggable target for host-oriented antimalarial interventions. *J Exp Med*. 2015;212(8): 1145-1151.

49. Chen ZN, Mi L, Xu J, et al. Targeting radioimmunotherapy of hepatocellular carcinoma with iodine (131I) metuximab injection: clinical phase I/II trials. *Int J Radiat Oncol Biol Phys*. 2006;65(2): 435-444.

50. Aniweh Y, Gao X, Hao P, et al. P. falciparum RH5-Basigin interaction induces changes in the cytoskeleton of the host RBC. *Cell Microbiol*. 2017;19(9):e12747.

2018 131: 1111-1121
doi:10.1182/blood-2017-08-802918 originally published online January 19, 2018

Disrupting CD147-RAP2 interaction abrogates erythrocyte invasion by *Plasmodium falciparum*

Meng-Yao Zhang, Yang Zhang, Xiao-Dong Wu, Kun Zhang, Peng Lin, Hui-Jie Bian, Min-Min Qin, Wan Huang, Ding Wei, Zhao Zhang, Jiao Wu, Ruo Chen, Fei Feng, Bin Wang, Gang Nan, Ping Zhu and Zhi-Nan Chen

Blood (print ISSN 0006-4971, online ISSN 1528-0020), is published weekly by the American Society of Hematology, 2021 L St, NW, Suite 900, Washington DC 20036.